

MICROSTRUCTURE CHARACTERIZATION OF POROUS MICROALLOYED ALUMINIUM-SILICATE CERAMICS

J. Purenović^{*#}, V. V. Mitić^{*, **}, V. Paunović^{*}, M. Purenović^{***}

^{*}Faculty of Electronic Engineering, University of Niš, Niš, Serbia

^{**}Institute of Technical Sciences, SASA, Belgrade, Serbia

^{***}Faculty of Sciences and Mathematics, University of Niš, Niš, Serbia

(Received 31 March 2011; accepted 27 April 2011)

Abstract

Kaolinite and bentonite clay powders mixed with active additives, based on $Mg(NO_3)_2$ and $Al(NO_3)_3$, sintered at high temperatures produce very porous ceramics with microcrystalline and amorphous regions and highly developed metalized surfaces (mainly with magnesium surplus). Microstructure investigations have revealed non-uniform and highly porous structure with broad distribution of grain size, specifically shaped grains and high degree of agglomeration. The ceramics samples were characterized by scanning electron microscopy (SEM), energy dispersive spectrometer (EDS), X-ray diffraction analysis (XRD) and IR spectroscopy analysis, prior and after treatment in "synthetic water", i.e. in aqueous solution of arsenic-salt. Grain size distribution for untreated and treated samples was done with software SemAfore 4. It has shown great variety in size distribution of grains from clay powders to sintered samples.

Keywords: Aluminium-silicate ceramics; Active additives; Microstructure; Microalloying; Grain size distribution.

1. Introduction

Ceramics are the newest class of tool materials with potential for a wide range of high-speed finishing operation. The development of current ceramic tool

materials was partially based on the advances in high-temperature structural ceramic materials and processing technology developed in the early 1970s. Ceramics are inorganic, nonmetallic materials that are subjected to high temperature during

[#] Corresponding author: jelena.purenovic@elfak.ni.ac.rs

synthesis or use. The use of ceramic tools in different fields of materials science is beginning to increase with the advent of alloyed ceramics and ceramic-matrix composites, as well as with the advances in ceramic processing technology.

The technology of ceramics is a rapidly developing applied science in today's world. Technological advances result from unexpected material discoveries. On the other hand, the new technology can drive the development of new ceramics. Currently many new classes of materials have been devised to satisfy various new applications [1].

Porous materials have fine pores (voids) and are used in filters for wastewater as well as in environmental detoxification components such as catalyst supports. While porous ceramics are conventionally manufactured by sintering raw ceramic powders at a non-densifying temperature, the maximum porosity obtainable is limited to approximately 50 - 60%. Higher porosity levels can be obtained by the addition of large quantities of pore formers such as resin beads and carbon, which are then removed by oxidation [2].

Alloying may be defined as the process of adding one or more elements or compounds to interact with the base compound in order to obtain beneficial changes in its mechanical, physical, or chemical properties or manufacturing/processing characteristics [3].

Synthesis of porous silicate ceramics causes significant interest in view of a wide spectrum of its use in various areas of techniques, chemistry, ecology, etc [4].

Modified aluminium-silicate ceramics,

alloyed with magnesium and microalloyed with aluminium, can be included in modern ceramics materials (functional and ecological ceramics). Specific area of this kind of ceramics is highly developed, with very large number of macro, mezzo, micro and submicro pores. Because of the large number of pores, porous ceramics have enormous surface areas, and so can make excellent catalysts.

Natural clays such as kaolinite and bentonite, which are natural colloidal, hydrated aluminium silicates, have the greatest application in catalysts technology. They are used as ion exchangers to remove different types of pollutants in water treatment, mostly to adsorb heavy metal ions, due to high cationic exchange capacity [5-8]. Therefore, this particular kind of clay was chosen to act, in its ceramic form, as the support substrate for magnesium aluminium silicate catalyst.

Porous ceramics made of mixture of natural kaolinite and bentonite clay exhibit crystalline areas, the most probably of zeolite structure, although the most of the ceramics bulk are made of amorphous oxides of Fe and alkaline metals. The oxides mixtures and metalized amorphous ceramics regions show high electrochemical and chemical activities in contact with water, which make it "active" ceramics. The possibility for removal of heavy metal cations, and other ions and radicals present in the treated water makes this ceramics a very powerful tool for processing of drinking water and sewage disposal of waste waters [9].

The main goal of this work is to examine microstructure and characteristics of Mg-

enriched kaolinite-bentonite clay ceramics, prior and after treatment with aqueous solution of arsenic salt, and also to determine grain size distribution prior and after sintering process. Removal of arsenic from its water solution was estimated by using EDS analysis.

2. Experimental

Porous alloyed and microalloyed ceramics was obtained by chemical and thermal transformations of natural kaolinite and bentonite clay. After collection, stones and other heavy particles were removed from clay sample. After milling, clay powder and active components were homogenized and pressed. Sodium silicate water solution was used to obtain a viscosity suitable for granulation, and $(\text{NH}_4)_2\text{CO}_3$ was added to achieve supplementary porosity during sintering process. Alloying was accomplished with water solution of $\text{Mg}(\text{NO}_3)_2$ (2-10 wt%) and microalloying with water solution of $\text{Al}(\text{NO}_3)_3$. The plastic clay mass was reworked into pellets, 10-15 mm in diameter on average and 3-4 mm of thickness. The pellets were dried at 200°C for 3-4 hours and sintered for 30 min at 600°, 700°, 800°, 900° and 1100°C and subsequently cooled to room temperature. Cooled sintered pellets were kept in closed plastic container to avoid undesired adsorption of chemicals or water. All chemicals used were from Merck p.a. Sintered samples were treated in a glass beaker for 24 and 48 hours in 20 ml of “synthetic water”, i.e. in aqueous solution of arsenic salt. Aqueous solution of arsenic (V), of concentration 500 mg l^{-1} , was prepared by

dissolving $\text{Na}_2\text{HAsO}_4 \cdot 7\text{H}_2\text{O}$ (Fluka AG, Buchs SG, Switzerland, p.a.) in distilled water. After the period of treatment, the ceramics samples were rinsed with distilled water, at first dried at room temperature on filter paper and then at 180°C for one hour. The as prepared samples were used for the characterization of the materials properties.

Different methods of analysis were used for the characterization of ceramics samples [10]. The microstructures and micro morphology of the as sintered samples were observed by scanning electron microscope (SEM-JEOL-JSM 5300). Prior to examination the specimens' surface was sputtered with gold. The software SemAfore 4 was used for analysis of photomicrographs with goal to obtain grain size distribution. The compositional analysis was performed using energy dispersive spectrometer with beam controller (EDS-LINK QX 2000 analytical). Mineralogical structural composition was determined by XRD analysis. X-ray diffraction patterns, for identification of crystalline phases, were collected on XRD SIEMENS D-500 type diffractometer, operating with Ni-filtered $\text{CuK}\alpha$ radiation. For additional information on chemical structure of magnesium aluminium silicate ceramics before and after contact with arsenic aqueous solutions, IR spectroscopy analysis (FTIR spectrophotometer Win Bommem 100, Germany) was carried out. The specimens for the analysis were prepared by standard potassium bromide technique for solid probes in a hydraulic press. The density of samples was determined by Archimedes method.

3. Results and discussion

The morphology of the sintered samples indicates non-uniform ceramics structure, inhomogeneous surface and particles varying in shape and exhibiting the degree of agglomeration. SEM images, used for determination of particle size are represented at Figs. 1, 3 and 5. Using automatic image analysis, SemAfore 4, it was possible to measure the grains size (minimum, maximum and average values), as well as the distribution of grains sizes. At least 150 grains, located on different specimens, were measured for particle size distribution.

Microstructure revealed a quite porous ceramics with a heterogeneous grain size distribution. SEM analysis of the pre-reacted

powders (Fig. 1) showed that the average particle size is of the order $10\mu\text{m}$, while there are also observed smaller particles, as well as a only few agglomerates of greater size, up to several tens of micrometers. The cumulative grain size distribution curves for these samples are represented at Fig. 2.

After the sintering process, the grain size of powdered samples with 6 wt% sintered at 600°C , prior and after 24h treatment in "synthetic water", (Fig. 3), decreases. Almost 70% of grains are with the size less than $2\mu\text{m}$ and the average particle size is in the range about $4\mu\text{m}$, as can be seen at Fig. 4.

The same analysis for sintered samples, (Fig. 5), showed insignificant difference in average grain size in comparison with

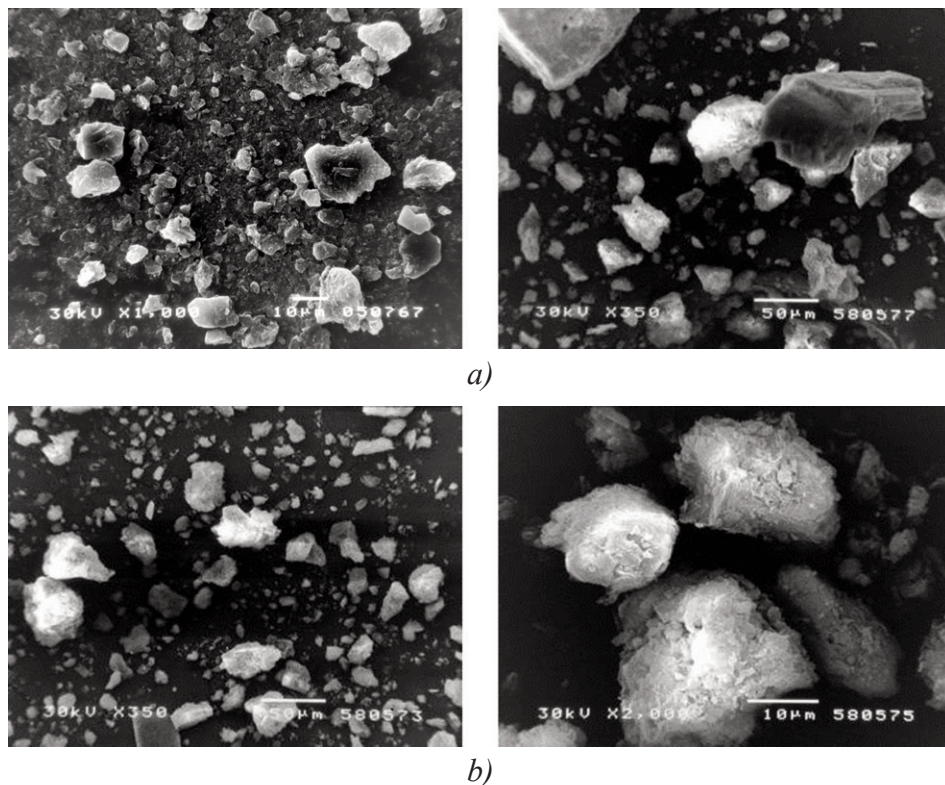


Fig. 1. SEM microphotographs of: a) kaolinite and bentonite clay powder and b) kaolinite and bentonite clay powder with $\text{Mg}(\text{NO}_3)_2$ and $\text{Al}(\text{NO}_3)_2$ as active additives.

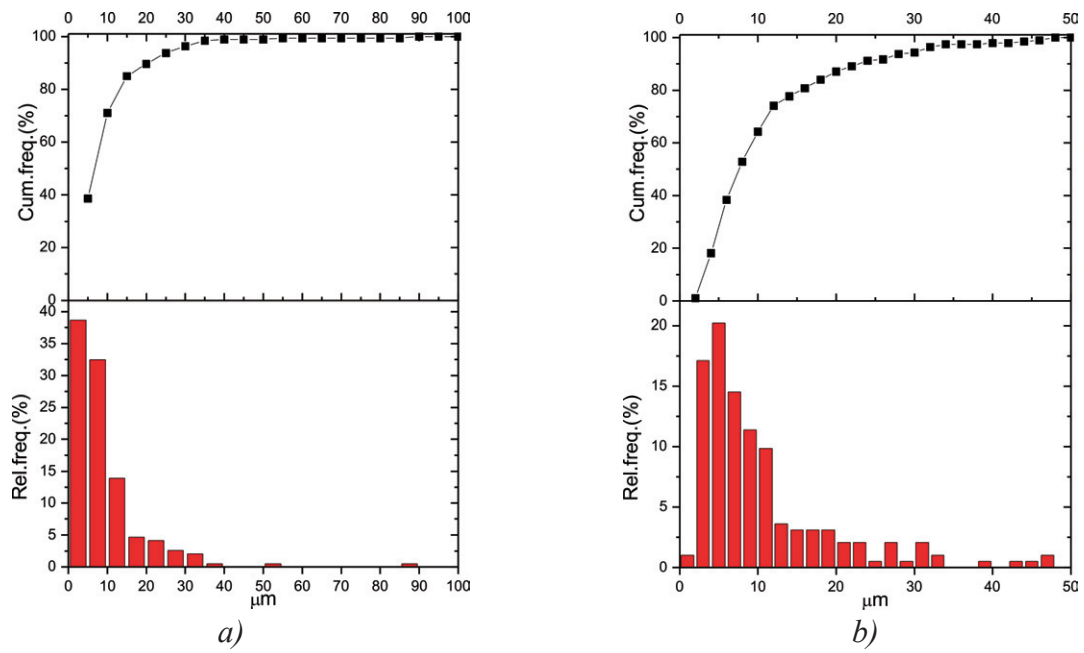


Fig. 2. Cumulative grain size distribution curves for: a) clay powder and b) clay powder with active additives.

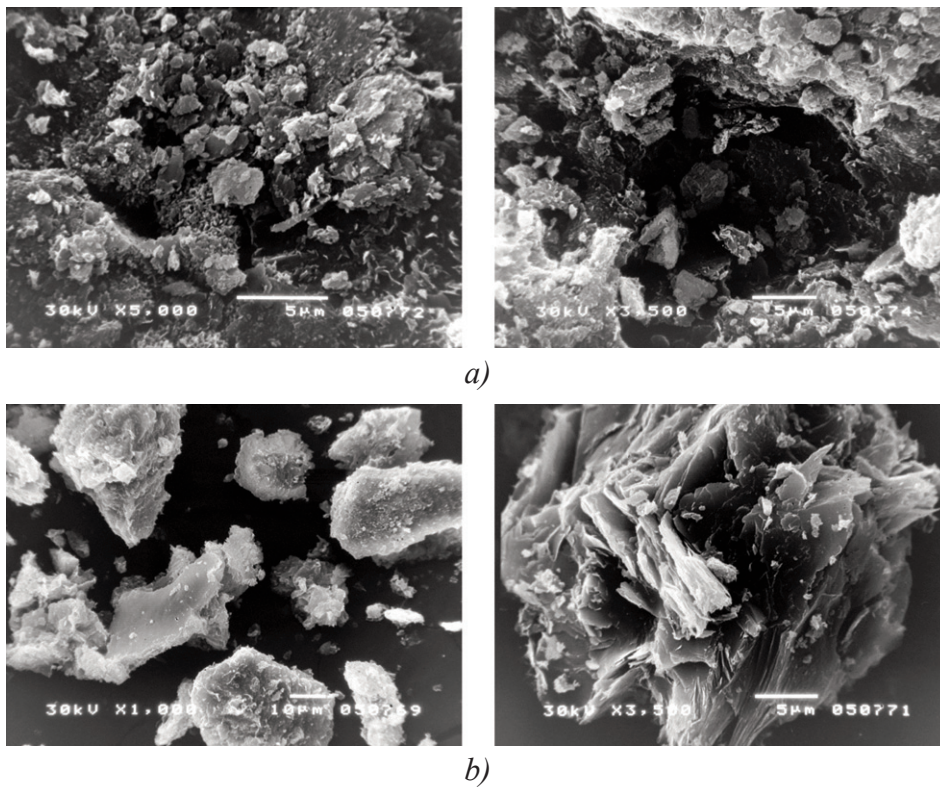


Fig. 3. SEM microphotographs of powdered sample with 6 wt% of active additive sintered at 600°C: a) untreated and b) treated for 24h in "synthetic water".

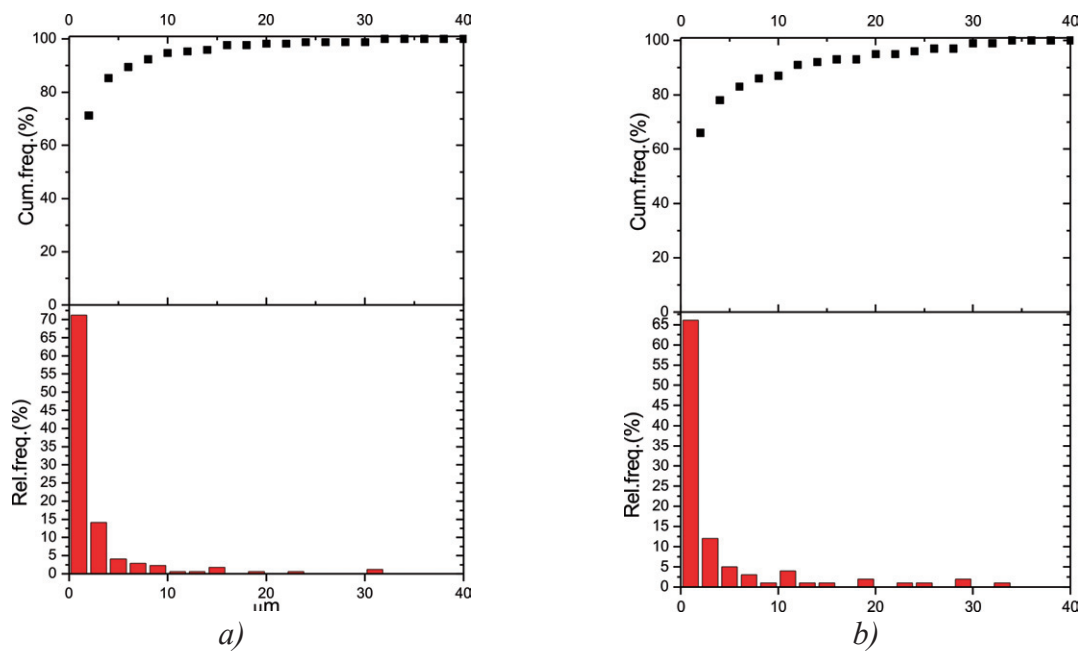


Fig. 4. Cumulative grain size distribution curves for powdered sample with 6 wt% of active additive sintered at 600°C: a) untreated and b) treated for 24h in "synthetic water".

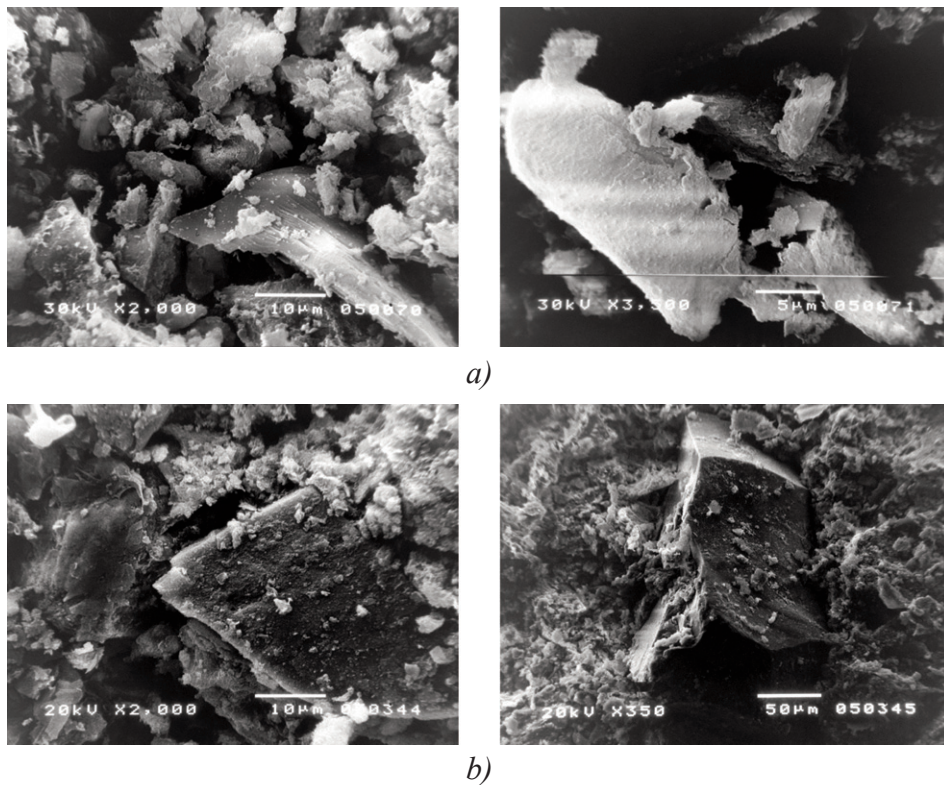


Fig. 5. SEM microphotographs of sample with 6 wt% of active additive sintered at 600°C: a) untreated and b) treated for 24h in "synthetic water".

powdered samples. Grain size distribution curves, illustrated in Fig. 6, showed that the greatest percentage of particles (about 30%) have sizes up to 4µm, while the less percent of particles have sizes up to 15 µm and some

agglomerated particles up to 30 µm [11-13].

Statistical calculations of grain size for all investigated samples are given in Table 1.

Beside well known phenomena and processes during materials sintering, alloyed

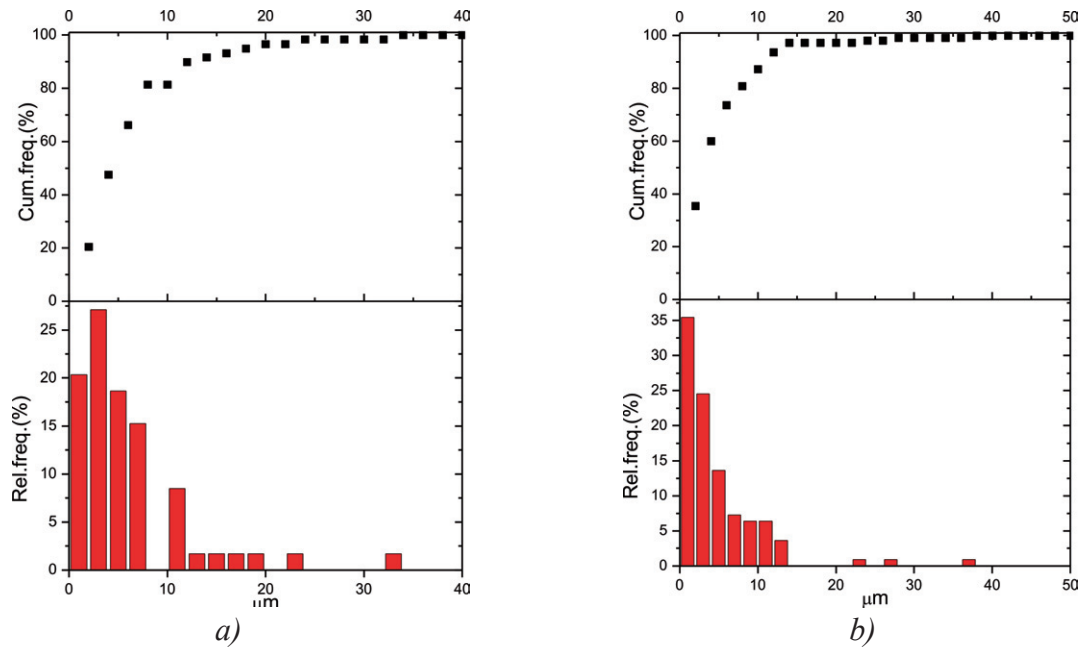


Fig. 6. Cumulative grain size distribution curves for sample with 6 wt% of active additive sintered at 600°C: a) untreated and b) treated for 24h in “synthetic water”.

Table 1. Statistical calculation of grain size.

SAMPLE	Mean particle size (µm)	Maximum particle size (µm)	Minimum particle size (µm)
Clay powder	9.27686	85.3	0.58
Powder of clay with active additives	10.3585	46.9	1.44
Powder of sample 6 wt%/600°C	2.67436	30.4	0.17
Powder of sample 6 wt%/600°C/24h	4.02931	33.8	0.203
Sintered sample 6 wt%/600°C	5.99373	32.9	0.78
Sintered sample 6 wt%/600°C/24h	4.876	36	0.575

and microalloyed porous aluminium-silicate ceramics has some specificities. Magnesium and aluminium, as alloying and microalloying elements respectively, on account of decomposition of starting nitrates, cover the grains with amorphous metal and oxide films. Thus, the greater dispersity of microcrystalline grains is conditioned, as well as the change of stoichiometric composition, spot defects and dislocations. On the other side, due to large concentration of dislocations and present additives, i.e. alloying and microalloying elements, fragmentation of bigger grains to large number of smaller grains occurs. These grains are also overtaken with amorphous metal and oxide films. On the temperature of sintering and phase transformations, decomposition of $Mg(NO_3)_2$ and $Al(NO_3)_3$ on metals and gaseous NO and NO_2 , is the cause of great intensions of gaseous phase in capillaries. All mentioned processes affect on porosity of ceramics and fragmentation of

bigger grains to several smaller grains. Therefore, the microstructure of ceramics is porous, highly amorphous and finely crystalline. The new procedure of alloying and microalloying [9, 14], which implies the change of microstructure and structurally sensitive properties, is exact approval for facts and phenomena mentioned above.

The qualitative chemical composition of samples was estimated from EDS spectra. They pointed out a wide range of oxides-Mg, Al and Si oxides are dominant in ceramics structure, while the oxides of other present elements are in traces. SEM image of sample treated for 48 hours in “synthetic water” (Fig.7) revealed very interesting crystallographic form of grains. Application of localized EDS beam (cross section area of $5 \mu m^2$) to these specifically shaped grains, (flower like), confirmed that they were arsenic entities, i.e. new phases or clusters of arsenic, with the highest concentration of deposited arsenic. The La_1 X-ray peak of

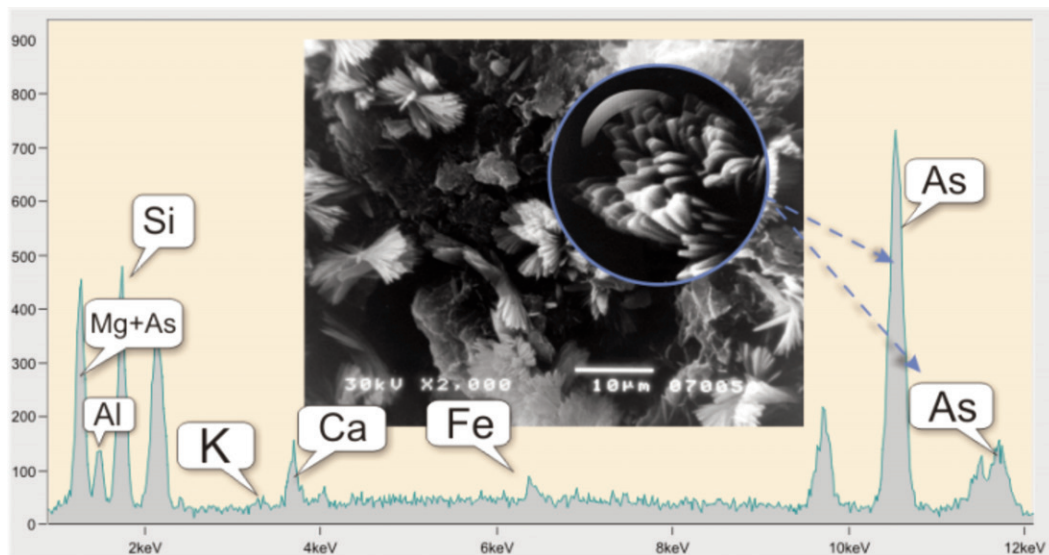


Fig. 7. SEM/EDS image of samples with 6 wt% of $Mg(NO_3)_2$ sintered at $800^\circ C$, treated for 48h in “synthetic water”.

arsenic was detected in EDS spectra and it can be concluded it is dominant. That leads to the conclusion that during the interaction of ceramics with “synthetic water” the arsenic was adsorbed and incorporated in its structure.

XRD technique for characterization of microstructures was used to determine the percentages of various phases present in a specimen if they have different crystal structures. XRD analysis of clay powders mixed with active components (Fig. 8) revealed more about phase composition of the ceramics, i.e. the presence of anorthite $\text{CaAl}_2\text{Si}_2\text{O}_8$ (JCPDS 20-0020), albite $\text{NaAlSi}_3\text{O}_8$ (JCPDS 20-0572) and palygorskite (hydrated magnesium aluminium-silicate) $(\text{Mg,Al})_5(\text{Si, Al})_8\text{O}_{20}(\text{OH})_{28}\text{H}_2\text{O}$ (JCPDS 21-0957), as major minerals. Anorthite is most dominant mineral phase, while albite and palygorskite are in the less percent present. Peaks present in the diffractograms were identified with the aid of JCPDS cards. Crystallographic composition of powders of

sintered ceramics sample, before and after treatment in “synthetic water” (Fig. 9 and Fig. 10) show dominant presence of crystalline phases of anorthite and albite. The existence of crystal modifications in, otherwise, amorphous structure of porous modified aluminium-silicate ceramics is confirmed in that way.

The IR spectrum represented at Fig. 11 is typical for combination of several crystalline and amorphous aluminium silicates, the most of them probably: feldspat (albite like structure: $428\text{--}650$; $720\text{--}790$ and $992\text{--}1155\text{ cm}^{-1}$); kaolin (magnesium-aluminium silicate with characteristic Mg-oxide peak around 790 cm^{-1}); strongly adsorbed waters ($1625\text{--}1635$ and $3200\text{--}3280\text{ cm}^{-1}$) and crystalline water (around 3200 cm^{-1}). After prolonged contact of the ceramics with water, the IR spectrum of the same surface changes (Fig. 12). Loss of the fine spectrum structure seen in Fig. 11 is obvious, particularly from 1089 cm^{-1} towards high wave numbers, the most probably as a

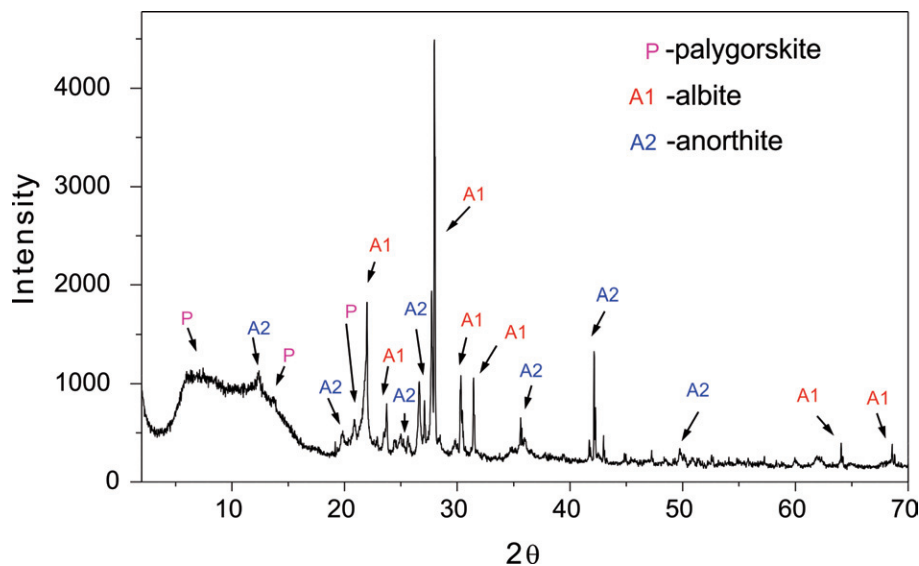


Fig. 8. XRD diffractogram of clay powders mixed with active components.

consequence of the chemical changes induced to the ceramic surface and stronger bonds of the water molecules and OH-groups with Al, Mg, Ca, K, Si and Fe cations [15].

The apparent density of ceramics samples

(Fig. 13) determined by means of Archimedes technique, decrease with the increase of sintering temperature and the amount of active additives. It is in accordance with the density of solid samples based on clay, with $\rho_s=2.5-2.7 \text{ g/cm}^3$ [16].

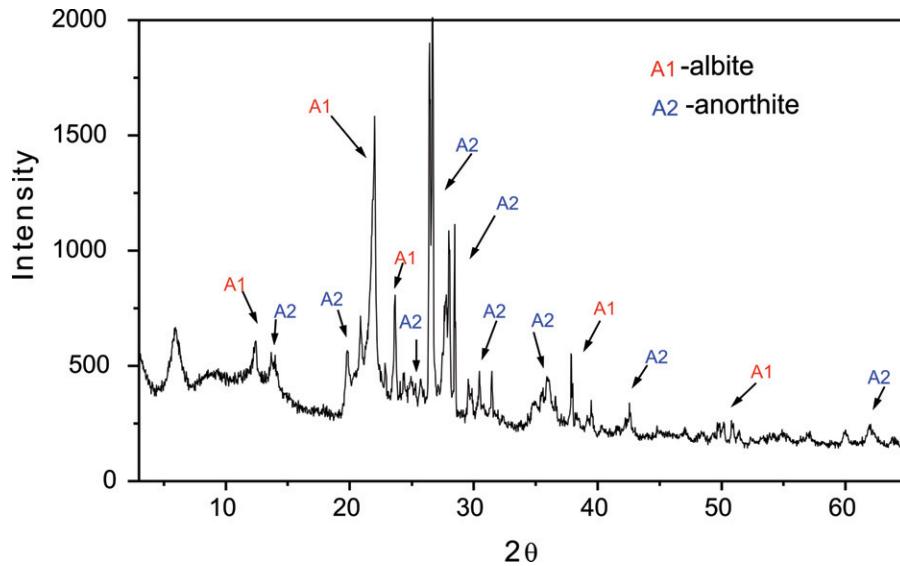


Fig. 9. XRD diffractogram of powder of untreated ceramics samples with 6 wt% of active additive sintered at 900°C.

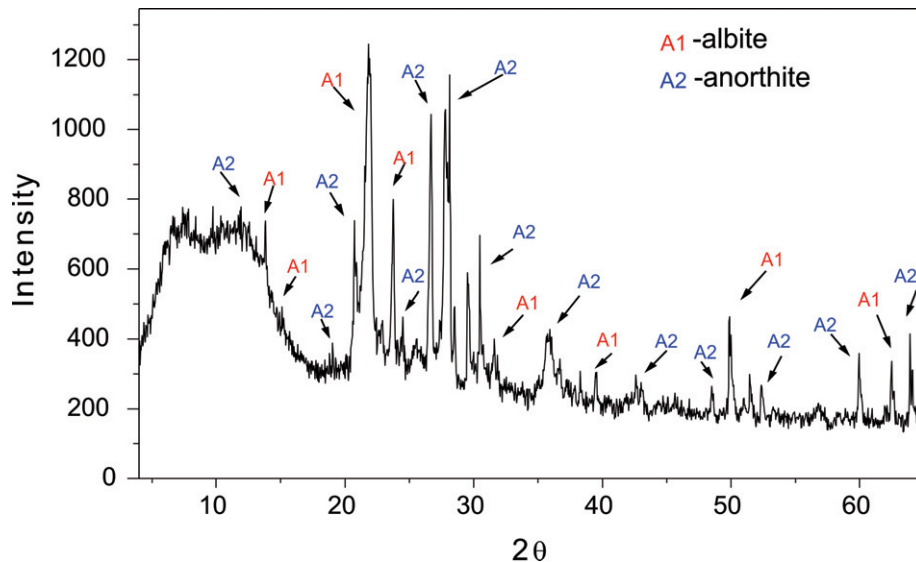


Fig. 10. XRD diffractogram of powder of ceramics samples with 6 wt% of active additive sintered at 900°C, treated for 24h in "synthetic water".

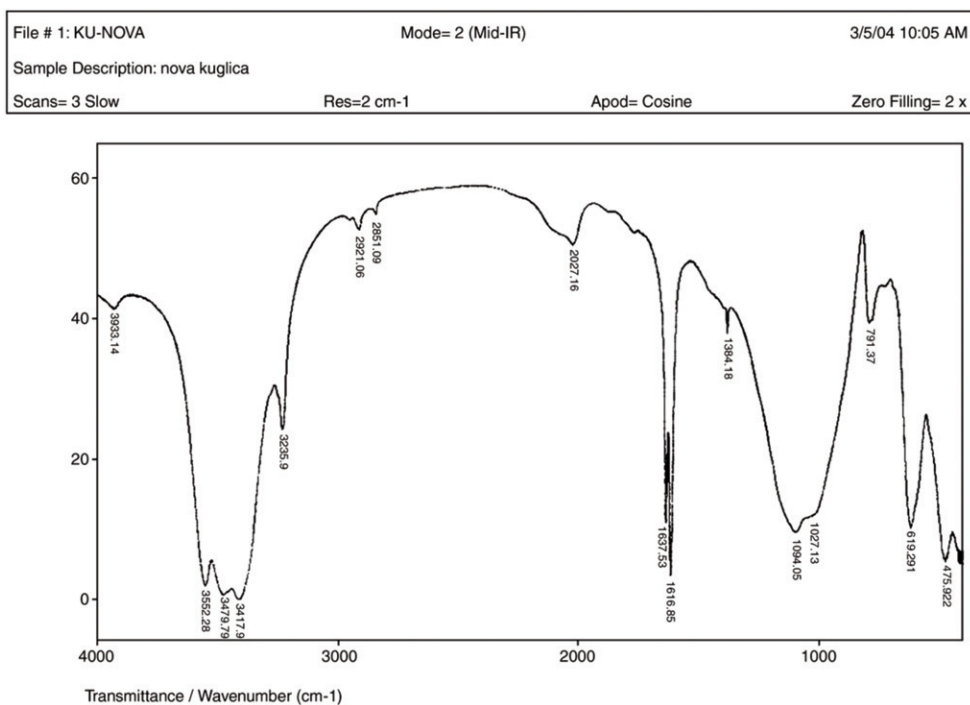


Fig. 11. An IR spectrum of untreated magnesium aluminium silicate ceramics sample.

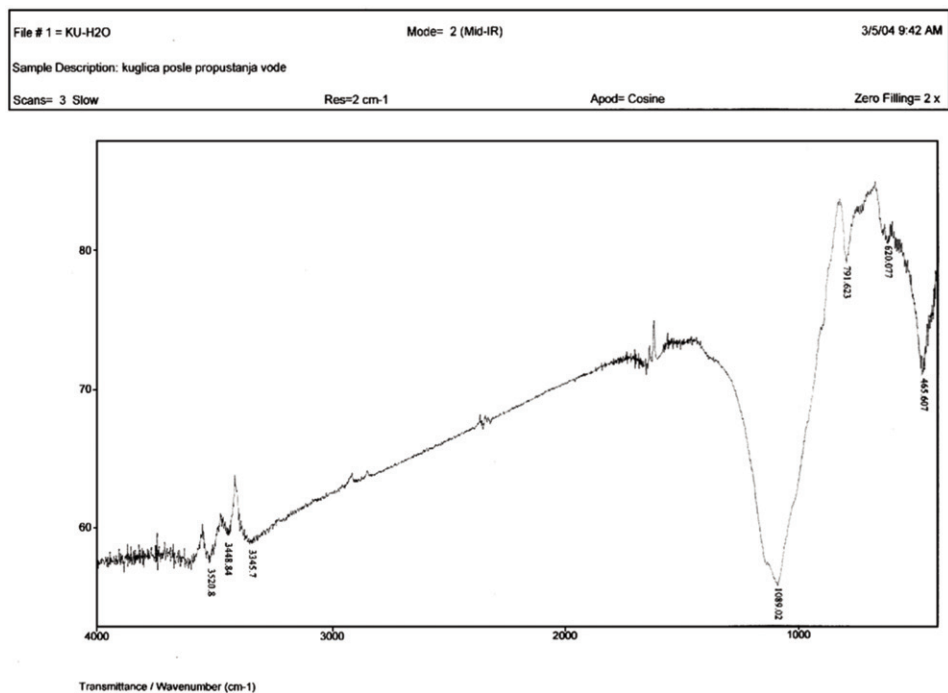


Fig. 12. An IR spectrum of magnesium aluminium silicate ceramics sample treated for 24h in "synthetic water".

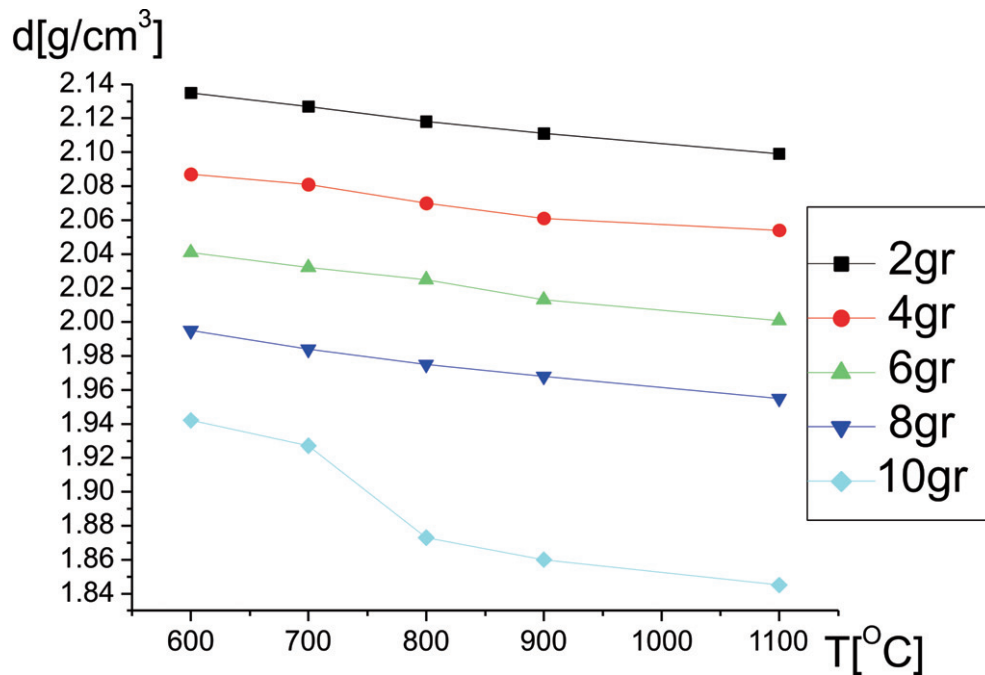


Fig. 13. Density of untreated samples in function of sintering temperature.

4. Conclusions

Aluminium-silicate ceramics modified with magnesium exhibits very porous amorphous structure, with appreciate portion of crystalline grains sited in magnesium and aluminium silicates matrix. Microalloying additives cause the formation of thin layers of magnesium and aluminium silicates on grains surface. Metals surplus, Al and Mg, make this ceramics unstable in contact with other medium. Magnesium enriched aluminium silicate ceramics exhibited highly developed surface area and porosity, zones of crystalline and amorphous structure and individual metal clusters scattered over the ceramics surface. Since microalloying additives are metals, metallization of ceramics grains occur. Observed porosity is most probably a result of gas evolution from decomposition of the active components

during the high temperature sintering.

There is a significant concentration of irregularly shaped large agglomerates, consisting of smaller particles, and also a large quantity of particles with different shapes and dimensions. That leads to the conclusion that this kind of ceramics has bimodal structure. Cumulative curves illustrated non-homogeneous grain size distribution. Sintering process caused decreasing of grains size. It happens due to fragmentation of grains on the account of decomposition of microalloying additives, followed by capture of gaseous phases in capillaries. Therefore, the large number of smaller grains is present in the sintered ceramics structure.

XRD diffractograms and IR spectra confirmed the crystalline modifications in mostly amorphous structure of porous modified aluminium-silicate ceramics. EDS

analysis showed the presence of adsorbed arsenic in ceramics structure, and hereby this kind of ceramics can be used for purifying of water sample from unwanted ingredients, such as heavy metal ions.

Acknowledgements

This research is a part of the project "Directed synthesis, structure and properties of multifunctional materials" (No. 172057). The authors gratefully acknowledge the financial support of Serbian Ministry for Science and Technological Development for this work.

References

1. M. Rosso, Ceramic and metal matrix composites: route and properties, Proc. XII International Scientific Conference, Achievements in Mechanical & Materials Engineering, Poland, 2003.
2. Y. Huang, K. Wang, D. Dong, D. Li, M. R. Hill, A. J. Hill, H. Wang, Microporous and Mesoporous Materials, 127 [3] (2010) 167.
3. W. Chen, J. Kong, W. J. Chen, J. Min. Metall. Sect. B-Metall., 47 [1] B (2011) 11.
4. Y. M. Enríquez Méndez, M. Vlasova, I. Leon, Ma. Trejo, M. Kakazey, Journal of the Australian Ceramic Society, 46 [1] (2010) 53.
5. K. O. Adebawale, I. E. Unuabonah, B. I. Olu-Owolabi, Applied Clay Science, 29 [2] (2005) 145.
6. Z. Zeng, J. Jiang, Int. J. Environ. Stud., 62 [4] (2005) 403.
7. Y. Kobayashi, K. Sumi, E. Kato, Ceram. Inter., 26 [7] (2000) 739.
8. S. Chandrasekhar, P. N. Pramada, Applied Clay Science, 27 [3-4] (2004) 187.
9. V. S. Cvetković, J. M. Purenović, M. M. Purenović, J. N. Jovičević, Desalination, 249 [2] (2009) 582.
10. G. B. Qiu, Y. Xu, J. Min. Metall. Sect. B-Metall. 46 [2] B (2010) 131.
11. Z. X. Yan, J. Deng, Z. M. Luo, Materials Characterization, 61 [2] (2010) 198.
12. A. L. Horovistiz, E. N. S. Muccillo, Journal of the European Ceramic Society, 31 [8] (2011) 1431.
13. M. Jayasankar, K. P. Hima, S. Ananthakumar, P. Mukundan, P. Krishna Pillai, K. G. K. Warriar, Materials Chemistry and Physics, 124 [1] (2010) 92.
14. V. S. Cvetković, J. M. Purenović, J. N. Jovičević, Applied Clay Science, 38 [3-4] (2008) 268.
15. R. L. Frost, A. M Vassallo, Clays and Clay Minerals, 44 [5] (1996) 635.
16. J. Raynal, M. Jullien, Clay Science, 12 [2] (2006) 52.